

The Determination of Fe, Si, and Al Content in Iron Ore Blast Holes by Nuclear Logging

M. Borsaru¹, A. Rojc¹, J. Ronaszeki², and C. Smith¹

ABSTRACT

Nuclear logging was tested for the in-situ determination of Fe, Si, and Al in iron ore blast holes with field tests at the BHP Billiton Iron Ore, Mount Waleback Mine. Prompt gamma neutron activation analysis (PGNAA) was used to determine percentages of Fe and Si while natural gamma logging was employed for the determination of Al. The accuracy given by nuclear logging is comparable to the accuracy provided by the laboratory analysis which was determined by taking the average of four samples collected from the cuttings deposited on the surface around the perimeter of a drill hole. The work also indicated that there is a chance of determining Al by PGNAA.

INTRODUCTION

Due to the deep penetration of neutrons and gamma rays, nuclear techniques are suitable for borehole logging applications and they are making inroads in the minerals industry. The benefits, which can be derived from nuclear logging, are:

1. It samples a much larger volume of the material surrounding the borehole than the sample taken for the laboratory analysis, thus providing better sampling statistics.
2. The results are available in real time.

Grade control at many Iron Ore Mines is conducted by sampling cuttings deposited on the surface in the form of a cone around the perimeter of a drill hole. Two samples are taken from each cone and are sent to the laboratory. There are errors associated with this sampling method that affects the sample accuracy. These are:

- collaring the hole (when mostly fine material is blown away from the hole)
- contamination of cuttings (as cuttings return from down-hole there is a contamination of returns and a resultant bias toward the top and middle of the hole)
- disruption to the cone (which takes place prior to the sample being taken thereby affecting the sample accuracy)
- inadequacy of sampling procedures during collection of the samples.

The down-hole logging is not affected by the processes listed above, as it analyses the surrounding rock in-situ.

The following example demonstrates the weight of ore sampled by the conventional sampling and nuclear logging for a typical production bench. The bench consists of a 10-meter regular grid of holes to a depth of 20 meters, intersecting ore of density 2.8-t/cubic meters. Consequently, each hole represents

an ore-block weighing 5,600 t. In conventional sampling, a sample of around 4 kg taken manually from the cone of drill cuttings represents the 5,600 t ore-block, giving a sample to ore-block ratio of approx. 1:1,400,000. The sampling radius of neutron-gamma is ~300 mm. For a 300 mm diameter blast hole, the mass of ore sampled by the neutron-gamma tool is approximately 32 t. Consequently, the sample to ore-block ratio for the neutron-gamma is about 1:175 which is much more favourable than for the conventional method.

Spectrometric borehole logging circumvents the problems of sampling inaccuracies and bottlenecks in data recovery. The logging data obtained can be used as a basis for dynamically scheduling of different sections of the mined ore.

CSIRO Exploration and Mining has developed the spectrometric nuclear logging system, SIROLOG, based on natural-gamma, gamma-gamma, and neutron-gamma techniques. In this system the whole gamma ray spectrum is recorded for each preset logging interval. By recording and analysing the whole gamma-ray energy spectrum from spectrometric measurement, one can extract more information from the logging data. A dedicated software package for spectrometric data analysis and interpretation has also been developed. The SIROLOG logging system has been commercialised and is available to the mining industry.

The paper presents the work carried out by CSIRO Exploration and Mining as part of a collaborative research agreement between CSIRO and BHP Billiton Iron Ore. The aim of the research was to determine whether nuclear logging is feasible for determination of Fe, Si, and Al content in iron ore blast holes.

Application of prompt gamma neutron activation analysis and natural-gamma to nuclear logging

When fast neutrons emitted by a neutron source enter a medium (e.g. iron ore), they undergo collisions with the nuclei present in the matrix and lose energy. If they are not absorbed during this slowing down process, they will ultimately reach the thermal energy of 0.025 eV. These thermal neutrons continue to diffuse through the medium until terminated by some other process, like neutron capture.

In the capture process, the thermal neutron enters the nucleus, and produces an unstable compound nucleus, which decays by emission of one or more γ -rays. The γ -rays are characteristic of the particular nucleus and are normally named neutron capture γ -rays. The neutron capture technique is commonly used in nuclear borehole logging and on-stream analysis, and its common name is prompt gamma neutron activation analysis (PGNAA).

Natural-gamma is another commonly used technique in nuclear logging. All rocks and soils contain a number of radioactive elements that emit gamma radiation. The three main sources of natural gamma rays are ⁴⁰K, which constitute 0.012% of total potassium and emits a single γ -ray of 1.46 MeV, decay products in the uranium series and decay products in the thorium

-
1. CSIRO Exploration and Mining, P. O. Box 883, Kenmore, Qld 4069, Australia
 2. BHPBilliton Technology, P. O. Box 188, Wallsend, N.S.W. 2287, Australia.

series. Shale is high in natural radioactivity while high-grade iron ore is very low in natural radioactivity, so natural gamma logging can be used to identify shale bands in iron ore. The alumina in iron ore is mostly associated with the presence of shale and it is likely that a correlation between alumina and natural gamma exists.

The basis for the determination of Fe and Si in this work is prompt gamma neutron activation analysis. Table 1 shows the neutron capture data for Fe, Si, and Al. This technique has been reported in earlier publications for in-situ determination of iron grade in iron ore (Loetsh, W., 1960; Eisler, P. L., et al., 1977; Charbucinski, J., 1993).

It is apparent from table 1 that the high-energy γ -rays released by the Al nuclei following neutron capture have practically the same energy as the γ -rays released by the iron nuclei. Due to the fact that the cross-section (σ) for neutron capture for Fe is an order of magnitude greater than for Al and the Fe concentration is larger than that for Al, the γ -rays of energy ~ 7.6 MeV are generated mostly by Fe. Hence, the Fe concentration is correlated with the count-rate of 7.6 MeV γ -rays recorded in the neutron capture spectrum and this is the basis for the determination of percentage Fe by neutron capture. However, the γ -rays of ~ 7.6 MeV generated by Al do interfere with the Fe measurement and affect the accuracy of Fe determination. The 6.02 and 5.92 MeV γ -rays released by Fe can also be used for measurement of %Fe.

The predominant γ -rays released by Si following neutron capture have energies of 4.9 and 3.5 MeV and the determination of %Si is based on their detection. Interference in the Si measurement comes from the 5.13 and 4.91 MeV γ -rays released by Al and from the Compton tails associated with the high intensity γ -rays released by Fe.

Table 1 shows that Al cannot be determined from the γ -rays released by Al nuclei following neutron capture. They are either too weak or swamped by the γ -rays released by Fe.

Another effect that must be considered when analysing neutron gamma spectra is inelastic scattering ($n, n'\gamma$) that takes place above the threshold energy, normally about 1 MeV. The neutrons produced by the neutron source have energies up to 8 MeV. Hence, when logging dry holes, a large number of fast neutrons impact on the iron ore because there are few hydrogen nuclei to slow them. During the slowing process, some of the fast neutrons interact with the ore by inelastic scattering. Table 2 shows the predominant γ -rays released by Al, Si, and Fe from neutron inelastic scattering.

As shown in the table, the energy of γ -rays produced by the neutron inelastic scattering is much less than the energy of γ -rays produced by neutron capture.

Instrumentation

Both the PGNA and natural-gamma logs were carried out with the same logging tool (the neutron source was not attached to the logging tool for natural gamma logging). The procedure was to log the holes for natural gamma radiation first, in case some detector components are activated by the neutron source.

The logging tool has a diameter of 100 mm manufactured from a carbon fibre composite material, uses a ^{252}Cf neutron source of strength 5 μg , and has a 75mm x 62mm diameter BGO

detector. The BGO detector and the neutron source were separated by 9 cm of lead to stop the gamma radiation emitted from the neutron source reaching the scintillation detector. A 4 cm spacer made of high-density polyethylene was also placed between the neutron source and the scintillation detector. The polyethylene contributes to the thermalisation of neutrons and produces a 2.2 MeV hydrogen peak in the capture spectrum, which is used to stabilise the gain. Gain stabilisation is especially important with BGO detectors, because of their extreme sensitivity to temperature variations. The BGO detector was covered with an aluminium cup coated with a 16-mg/cm² layer of ^{10}B (mixed with an epoxy resin) to shield the detector assembly from thermal neutrons.

Pulses produced by the gamma-ray detector are processed by a microprocessor incorporated in the probe and transmitted to the uphole computer. The full logging system consists of the probe, winch, SWISS (Single Wire Interface Supply System) interface, and a laptop computer.

Data analysis and interpretation

Multiple regression analysis was used to calibrate and test the accuracy of nuclear logging for the prediction of Fe, Si, and Al in dry iron ore blast holes. The method entailed setting windows in the gamma-ray spectrum and fitting a linear regression model of the form:

$$\text{Percent Fe (Si, Al)} = a_0 + a_1X_1 + \dots + a_nX_n,$$

where a_0, a_1, \dots, a_n are constants and X_1, \dots, X_n are count rate variables for the selected windows. The windows set in the gamma-ray spectrum were chosen to correspond to the Fe, Si, and Al γ -ray peaks. The determination of Al from natural-gamma logging was based on the regression of count rates in the natural gamma spectrum against %Al.

Field trials

The PGNA and natural gamma techniques were field tested at the BHP Iron Ore Mount Whaleback Mine. Eighty-seven blast holes were logged with both techniques. The holes were located in four areas: WB25N065 (57), WB24N166 (20), WB18N371 (5), and WB21N322 (5). Although the assumption was that the holes were dry, it was found that a number of holes were water-filled (the water level in some holes was $\sim 9\text{m}$). Only the dry sections of the holes were considered in the data analysis. Most holes were logged only once, but a few holes were logged twice to check the reproducibility of the logging techniques.

The dry holes were logged all the way to the bottom and four sample cuts were collected from each hole for chemical analysis. The chemical assay for the hole was obtained by taking the average of the four samples. These assays were used for calibration and comparison of nuclear predictions and laboratory analyses. Another two samples collected for production purposes (for 15 m depth) were also available, but they were not used in the data analysis. The chemical assays from only two areas (WB25N065 and WB18N371) were initially made available to CSIRO for calibration. The holes from the other two areas were used to compare the predictions from nuclear logging with the laboratory assays.

Results

Figures 1, 2a, and 2b show the natural-gamma and neutron-gamma spectra respectively integrated over the whole blast hole. A lithological log obtained from the total counts from natural gamma logging is shown in figure 3. The shale bands are characterised by high natural gamma count rates. Figure 4 shows the variation in the gamma-ray counts arising from hydrogen and iron nuclei for one blast hole following the neutron-capture process. It is apparent that areas with large iron content (high Fe γ -ray counts) have lower hydrogen content (low H γ -ray counts) and vice versa.

Comparison between nuclear predictions and laboratory assays

Chemical assays from 30 holes were used to calibrate the logging tool for Fe, Si, and Al. The calibration holes were selected according to the chemical assays such that the assays for Fe, Si, and Al covered the whole range from the lowest to the highest values and provided a good distribution of grades. Calibrations were obtained for Fe, Si and Al from the neutron-gamma logs and for Al (only) from the natural-gamma logs. While it was not anticipated that Al content could be accurately predicted from the neutron-gamma data, an attempt was made to obtain a calibration for Al from this data. The holes chosen for the calibrations were not necessarily the same for the three elements (Fe, Si, Al). Table 3 gives the root mean square (RMS) deviations (wt%) and correlation coefficients for Fe, Si, and Al given by the regression equations for the thirty calibration holes.

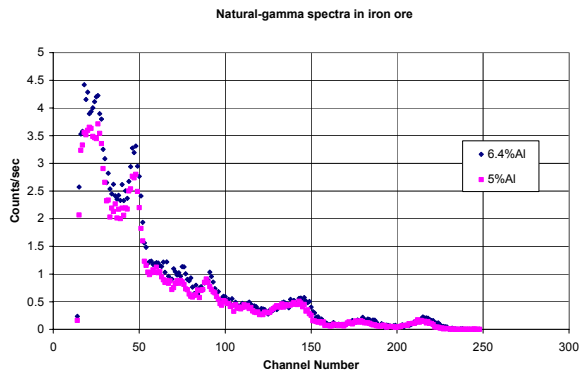


Figure 1: Natural-gamma spectra integrated over the whole hole in iron ore blast holes 70 (5%Al) and 66 (6.4%Al) in area

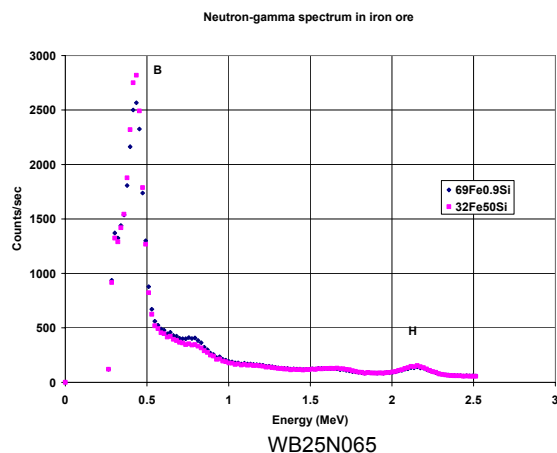
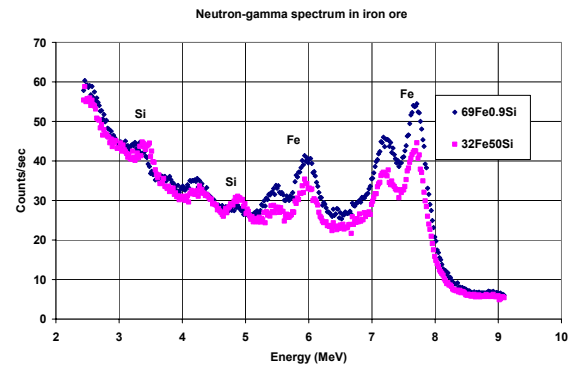


Figure 2a: Neutron-gamma spectra below 2.5 MeV integrated over the whole hole in iron ore blast holes 33, in area



WB25N065 (69%Fe, 0.9%Si) and 66, in area WB18N371 (32%Fe, 50%Si).

Figure 2b: Neutron-gamma spectra above 2.5 MeV integrated over the complete hole in iron ore blast holes 33, in area WB25N065 (69%Fe, 0.9%Si) and 66, in area WB18N371

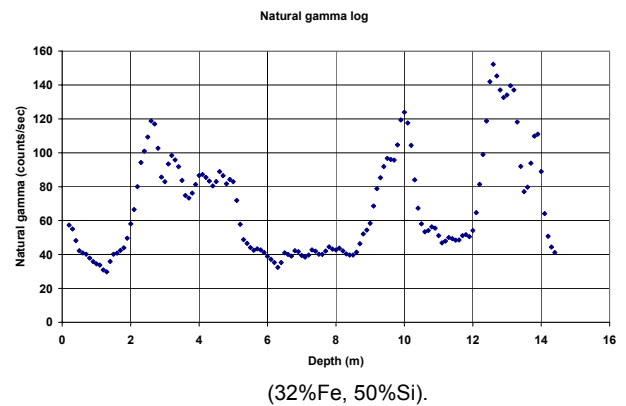


Figure 3: Total natural-gamma log in iron ore blast hole 12 in area

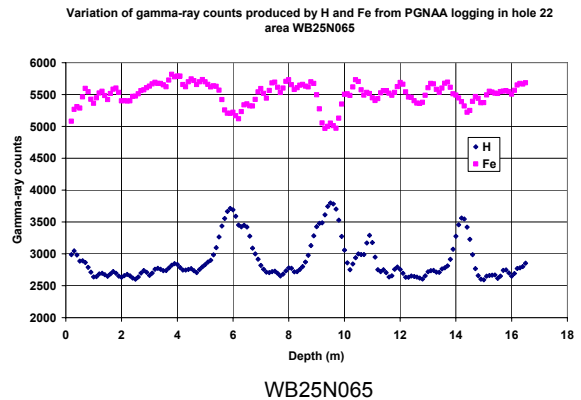


Figure 4: Variation of neutron-capture γ -ray counts produced by H and Fe in an iron ore blast hole

The regression equations derived for Fe, Si, and Al are listed in Table 4. Two regressions were derived for Fe and Si corresponding to wide and narrow ranges of variation, i.e. %Fe (31.7-69.5 and 59.1-69.5) and %Si (0.7-54 and 0.5-8.6).

As mentioned above, the energy windows shown in Table 4 were selected to correspond to Fe, Si, Al and H or combinations of these elements. The neutron capture spectrum is complex and the detector cannot fully separate the γ -rays according to their energies. An extra difficulty is the fact that the neutron flux generated by the ^{252}Cf neutron source is distorted in the orebody. One way to correct for this is to normalize the count rates recorded in the energy windows to the count rates recorded in the

H peak or the whole energy spectrum. The energy window 2000–2300 keV was set up to record the count rate in the hydrogen peak.

A second calibration equation for %Al was derived from the natural gamma logs as follows.

$$\%Al = -0.9 + 0.03 * Roi 1$$

where Roi (region of interest) 1 is the count rate in the window extending from channel 17 to channel 230. This corresponds to the total count rate in the natural gamma spectrum. The RMS deviation and the standard deviation of the population were 0.86 and 1.6 %Al respectively. The correlation coefficient was 86%.

Figures 5-8 show the cross-plots between chemical assays and nuclear predictions for Fe, Si, and Al given by the regression equations. The cross-plots for the wide range of variation for Fe and Si are only shown.

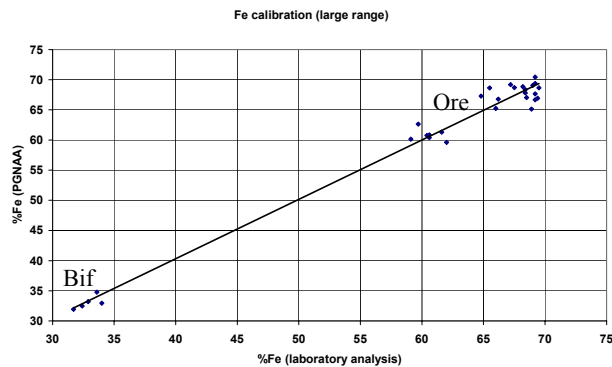


Figure 5: Chemical vs. neutron-gamma prediction of %Fe for wide Fe range

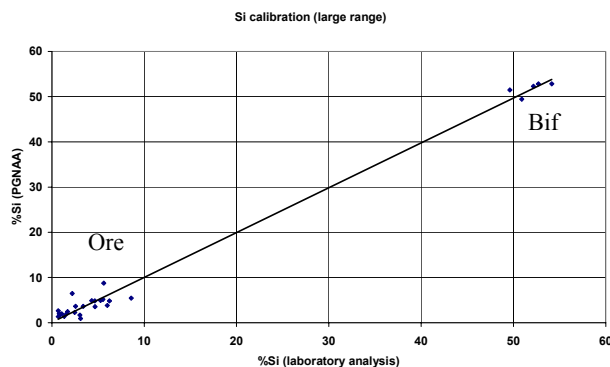


Figure 6: Chemical vs. neutron-gamma prediction of %Si for wide Si range

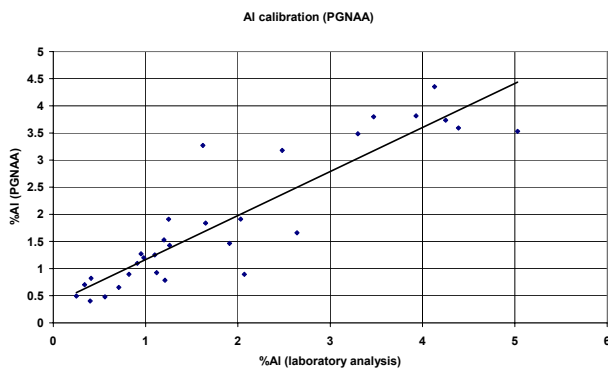


Figure 7: Chemical vs. neutron-gamma prediction of %Al

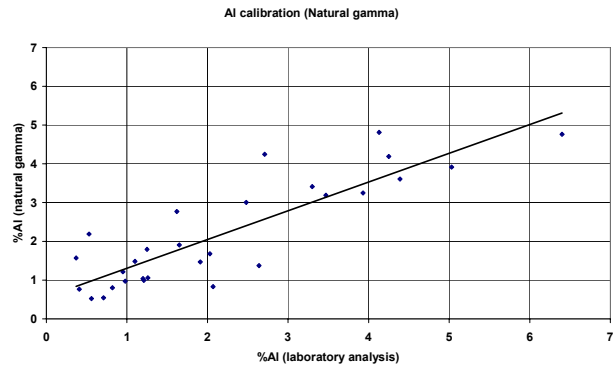


Figure 8: Chemical vs. natural-gamma prediction of %Al

The calibration equations given in Table 4 were used for predicting Fe, Si, and Al for the 'blind' holes logged in areas WB24N166 and WB21N322. A comparison between the nuclear predictions and laboratory assays averaged for the all holes logged in areas WB21N322 and WB24N166 are given in Table 5. Fe(lab) and Fe(prod) (columns 2 and 3) in Table 5 are the laboratory assays for the samples collected for the CSIRO field test (4 cuts) and the samples collected for production (2 cuts) respectively. "Fe(n-g) (column 3) lists the PGNAA predictions for Fe. Same notation is valid for Si and Al.

The depth of the logged holes was considered in the average. The table shows close agreement between the nuclear predictions and laboratory assays. The calibrations for Fe and Si obtained from the laboratory assays available for areas WB18N371 and WB25N065 were not able to predict the Fe and Si values for the holes 24, 55, and 62 (area WB21N322) because the Fe and Si values were outside the range of the calibrations. Values of 20% Fe and 50% Si were assumed for those holes.

Table 6 gives the RMS deviations σ between laboratory assays and nuclear predictions for all the holes that were not considered in the calibration equations. The RMS deviations were calculated using the formula

$$s = \sqrt{\frac{\sum_i (lab_i - nucl_i)^2}{2n}}$$

where lab_i and $nucl_i$ are the laboratory assay and nuclear prediction for the i^{th} hole and n is the number of holes.

Table 6 also shows that the RMS deviation for Al prediction using neutron capture is smaller than that for natural-gamma predictions. This is not well understood at this stage. One possible explanation is that the Al determination by neutron-gamma relies on the correlation that exists between Fe, Si, and Al. The fact that neutron-gamma was able to predict Al concentration with a better precision came unexpectedly and more work is needed to confirm those preliminary results.

Sources of errors

1. The Fe, Si, and Al assays for the holes selected for the calibrations must be known with high accuracy. The

predictions given by nuclear logging cannot be more accurate than the accuracy of assays used in the regression equations. Sampling is the largest source of errors affecting the laboratory assays. Although a sample consisting of four cuts taken from the cone improves the accuracy of assay compared to two cuts, the accuracy is still inferior to the samples obtained from cored or RC holes. The accuracy of the laboratory assays available for this field test was a major source of error.

2. Another source of errors arises from the fact that four cuts were collected to correspond to the full depth of the holes. However, a few holes were not dry and only the dry sections were considered for predictions or calibration.
3. Other sources of errors are related to the neutron-gamma technique, the most important being interference from other γ -rays produced in neutron- γ reactions.

In order to properly assess the accuracy of nuclear logging, the laboratory assays of the calibration holes must be known with higher accuracy than the assays available for the field tests described in this report.

Conclusion

The present work demonstrated that nuclear logging has the potential for in-situ determination of Fe, Si, and Al in iron ore blast holes. Fe and Si percentages are determined by prompt gamma neutron activation analysis (PGNAA) and the Al from the natural-gamma log. Two logs are therefore necessary for each hole. The time to log an 18 m hole is approximately 16-18 minutes, including the setting up and transport time from one hole to another hole. However, although not well understood, there is a chance of determining Al by PGNAA, and hence one log only would be needed per hole. More tests are needed to establish this.

It is difficult to assess the accuracy of the laboratory assays: the depths of the holes logged (four cuts were taken per sample) are different from the 15 m depth sampled for production (2 cuts taken per sample). However, looking at the assays for the individual cuts and production samples, the accuracy given by

nuclear logging looks comparable to the accuracy provided by the laboratory.

One important feature of nuclear logging is that it samples a much larger volume than the routine sample of approximately 4 kg taken from the cone. The sampling radii of the natural-gamma and neutron-gamma methods are 150 mm and 300 mm respectively. Hence, for a 300 mm blast hole 20 m deep, the masses of ore sampled by the natural-gamma and neutron-gamma tools are approximately 12 and 32 t respectively, which is much more representative than the 4 kg sample cut from the cones.

The determination of density was not one of the objectives in this work. However, if required, the density can be determined by the gamma-gamma technique. A combination natural-gamma / gamma-gamma tool must be employed for the simultaneous determination of the natural radiation (used for the determination of Al) and the backscattered gamma-gamma spectrum (for the density measurement). There is a slight possibility to determine the density from the neutron-gamma spectrum. This technique has been tested successfully for coal. However, it has never been tried in iron ore. Its viability can only be proved in a field test and cored holes assayed for density are required.

REFERENCES

- Charbucinski, J. 1993. Comparison of spectrometric neutron-gamma and gamma-gamma techniques for in situ assaying for iron grade in large diameter production holes. *Nuclear Geophysics* 7:133-141.
- Eisler, P. L., Huppert, P., Mathew, P. J., Wylie, A. W., and Youl, S. F. 1977. Use of neutron-capture gamma radiation for determining grade of iron ore in blast holes and exploration holes, in *Nuclear Techniques and Mineral Resources 1977*, pp215 (Proceedings Symposium IAEA: Vienna).
- Loetzsh, W., 1960. Neutron capture gamma ray spectroscopy for the exploration of iron-bearing ores in boreholes. *Kernenergie* 7(6/7):560.

Table 1: Neutron capture data for major components in iron ore.

Element (atomic mass)	Cross-section σ (barn)*	Major γ -rays (MeV)	γ -ray intensity (I) per 100 neutron radiative captures
Aluminium (26.98)	0.23	7.72	27.4
		7.69	4.2
		6.10	2.3
		5.13	2.6
		4.91	2.6
		4.69	3.9
		4.66	2.1
		4.13	6.4
Iron (55.85)	2.55	7.65	28.5
		7.63	24.1
		6.02	9
		5.92	9

Element (atomic mass)	Cross-section σ (barn)*	Major γ -rays (MeV)	γ -ray intensity (I) per 100 neutron radiative captures
Silicon (28.09)	0.16	7.2	7.8
		6.38	12.4
		4.93	62.7
		3.66	3.9
		3.54	68.0
		2.09	21.5
		1.16	19.9

*Thermal neutron capture

Table 2 Major γ -rays released by Al, Si and Fe from neutron inelastic scattering (normalised to a sample bulk density of 1.5 g cm⁻³).

Element	γ -ray energy (MeV)	Number of γ -rays in arbitrary units
Al	1.01	1066
	0.84	890
	2.21	493
Si	1.8	927
Fe	0.85	1709
	1.24	259

Table 3: Results from neutron-gamma logs

Parameter, range (%)	RMS deviation (wt%)	Correlation coefficient (%)	Standard deviation of the population (wt%)
Fe 59.1 – 69.5	1.2	97	3.7
Fe 31.7 – 69.5	1.7	99	12.9
Si 0.5 – 8.6	0.86	92	2.2
Si 0.7 - 54	1.7	99	18.6
Al 0.25 - 5	0.62	90	1.4

Table 4: Regression equations for Fe, Si, and Al from neutron-gamma logging; only two areas considered

Parameter, range (%)	Regression equation	Ratio 1 (R1) keV	Ratio 2 (R2) keV
Fe 59.1-69.5	%Fe=-304.3+373.6*R1+39*R2	(3100-5200)/(5200-8000)	(5300-8000)/(2000-2300)
Fe 31.7-69.5	%Fe=178.3-209.9*R1+14.6*R2	(3100-5200)/(5200-8000)	(5300-8000)/(2000-2300)
Si 0.5-8.6	%Si=202.2-32.7*R1-189.5*R2	(3100-5200)/(2000-2300)	(3100-5200)/(5200-8000)
Si 0.7-54	%Si=-320.6+37.3*R1+697.4*R2	(7500-7900)/(2000-2300)	(4600-5200)/(5200-6400)
Al 0.25-5	%Al=41.1-25.1*R1-14.9*R2	(4000-5200)/(2000-2300)	(4000-5200)/(5200-6400)

Table 5: Comparison of averaged laboratory assays and nuclear predictions for areas WB21N322 and WB24N166

Area	Fe (lab)	Fe (prod)	Fe (n- γ)	Si (lab)	Si (prod)	Si (n- γ)	Al (lab)	Al (prod)	Al (nat- γ)	Al (n- γ)
WB21 N322	38	36.9	32	32.2	38.1	39.4	4.9	4.9	3.7	4.7
WB24 N166	65	65.7	66	2.85	2.2	2.3	1.9	1.6	2.5	1.8

Table 6 RMS deviations between laboratory assays and nuclear predictions

RMS deviation	Fe(n- γ)	Si(n- γ)	Al(nat- γ)	Al(n- γ)
s	1.8	1.2	0.93	0.72
Range (%)	59.1-69.3	0.6-6.1	0.3-7.3	0.3-7.3